The Drosophila MLR COMPASS-like complex regulates *bantam* miRNA expression differentially in the context of cell fate

David J. Ford[1], Claudia B. Zraly[1], John Hertenstein Perez[1§] and Andrew K. Dingwall[1,2,*]

[1]Department of Cancer Biology, Stritch School of Medicine, Loyola University Chicago, Maywood, Illinois, 60153, [2]Department of Pathology & Laboratory Medicine, Stritch School of Medicine, Loyola University Chicago, Maywood, Illinois, 60153

[§]Current address: Public Health Institute of Metropolitan Chicago, IL

[*]Author for correspondence: Andrew K. Dingwall, PhD. Department of Cancer Biology, Stritch School of Medicine, Loyola University Chicago. Maywood, IL, USA 60153. Ph (708) 327-3141. adingwall@luc.edu

Keywords

Enhancers, Development, Drosophila, Differentiation, miRNA

Word Count (6625)

ABSTRACT

The conserved MLR COMPASS-like complexes are histone modifiers that are recruited to enhancer regions by a variety of transcription factors where they monomethylate histone 3 lysine 4, an epigenetic mark associated with gene activation. A critical *in vivo* target of the Drosophila MLR complex is the *bantam* miRNA that promotes cell proliferation and differentiation, and functions in feedback regulation of cellular signaling pathways during development. Loss of Drosophila MLR complex functions in developing wing and eye imaginal discs result in growth and patterning defects that are sensitive to *bantam* levels. Consistent with an essential regulatory role in modulating *bantam* transcription, the MLR complex binds to tissue-specific *bantam* enhancers and contributes to fine-tuning expression levels during larval tissue development. In wing imaginal discs, the MLR complex attenuates *bantam* enhancer activity by negatively regulating expression; whereas in eye discs, the complex exerts either positive or negative regulatory activity on *bantam* transcription depending on cell fate. Furthermore, the MLR complex is not required to control *bantam* levels in undifferentiated eye cells anterior to the morphogenetic furrow. Rather, the MLR complex serves to establish critical enhancer control of *bantam* transcription in undifferentiated eye cells for later regulation upon differentiation. Our investigation into the transcriptional regulation of a single target in a developmental context has provided novel insights as to how the MLR complex contributes to the precise timing of gene expression.

INTRODUCTION

COMPASS-like complexes (Complex of Proteins Associated with Set1) are highly-conserved chromatin modifiers responsible for methylation of the lysine 4 residue of histone 3 (H3K4), an epigenetic modification associated with active chromatin (Shilatifard 2012). While yeast contains a single COMPASS complex, multicellular eukaryotes harbor multiple orthologous complexes specialized for specific genomic targets and methylation activity. Those containing methyltransferases KMT2C (MLL3) or KMT2D (MLL2/4) in humans and Trr in Drosophila are part of a branch of COMPASS-like complexes that we refer to as MLR complexes (Fagan and Dingwall 2019). MLR complexes are recruited to transcription enhancer regions by a variety of binding partners where they catalyze the deposition of H3K4me1, and contribute to the removal of H3K27me3 and recruitment of the histone acetyltransferase p300/CBP (Issaeva et al. 2007; Herz et al. 2012; Hu et al. 2013; Wang et al. 2016; Lai et al. 2017). Enhancers, also known as cis-regulatory elements, propagate transcription factor signals and control gene expression in part by forming contacts with target promoters and dramatically increasing transcription efficiency (Levine 2010). This mechanism allows for the intricate patterns of spatiotemporal control of gene expression necessary for the normal development of most eucaryotes. Consequently, MLR complex regulation of enhancer activity is necessary for proper lineage determination, cellular differentiation, tissue patterning, and organismal development (Chauhan et al. 2013; Lee et al. 2013; Ford and Dingwall 2015; Ang et al. 2016; Wang et al. 2016), as well as embryonic stem cell differentiation (Wang et al. 2016). The loss of MLR complex functions are causally associated with developmental disorders or lethality in multiple animal species (Sedkov et al. 1999; Andersen and Horvitz 2007; Chauhan et al. 2012; Van Laarhoven et al. 2015). For example, in humans germline mutations of both *KMT2C* and *KMT2D* are foundational to

Kleefstra and Kabuki developmental disorders, respectively (Ng et al. 2010; Kleefstra et al. 2012); *KMT2C* and *KMT2D* are also two of the most frequently somatically mutated genes in a wide variety of human cancers, and identified as drivers of malignancy in some tumor types (Ford and Dingwall 2015). Previous work by our lab and others has determined that depletion of MLR complex subunits in Drosophila larval imaginal discs results in adult organ malformation affecting tissue size and patterning. Notably, MLR complexes have been demonstrated to interact with and be necessary for proper elaboration of multiple developmental signaling pathways, and evidence suggests that alterations of Dpp/TGF-β, Hippo, and Notch signaling underlie these phenotypes (Sedkov et al. 2003; Chauhan et al. 2012; Chauhan et al. 2013; Kanda et al. 2013; Qing et al. 2014).

We sought to better understand how the MLR complex regulates critical gene enhancers and how alteration of this activity leads to disease states by examining its function in a developmental context. In Drosophila, the MLR complex contributes to the positive regulation of the expression of Tgf-β paracrine signaling molecule Dpp during wing development (Chauhan et al. 2013), and Trr physically interacts with the coactivator Spen/SHARP on Notch signaling targets (Oswald et al. 2016). The MLR complex also associates with the Hippo coregulator HCF and signaling effector Yorkie for proper Hippo pathway target gene activation (Oh et al. 2014; Nan et al. 2019). In the fly, these developmental signaling pathways are all linked by the miRNA *bantam*, which is a direct transcriptional target as well as a feedback regulator of these three pathways through translation inhibition of pathway components Mad, Tgi/SdBP, and Numb (Oh and Irvine 2011; Shen et al. 2015; Wu et al. 2017; Kane et al. 2018). Defects resulting from alteration of these developmental pathways can be rescued or enhanced through modulation of *bantam* levels, and *bantam* overexpression or depletion alone leads to disrupted tissue formation

(Hipfner et al. 2002; Brennecke et al. 2003; Nolo et al. 2006; Peng et al. 2009; Becam et al. 2011; Herranz et al. 2012).

The *bantam* miRNA is generated from a ~12kb non-coding precursor RNA *(CR43334)* and the *bantam* locus spans nearly 40kb that includes multiple tissue-specific enhancers responsible for regulating proper expression levels (Oh et al. 2013; Slattery et al. 2013). The best characterized biological function of *bantam* is within the Hippo pathway, where it serves to promote cell proliferation and inhibit apoptosis through translation inhibition of the proapoptotic gene *hid* (Brennecke et al. 2003). The Yorkie (Yki) transcription factor forms heterodimers with either Scalloped (Sd) or Homothorax (Hth) to directly regulate tissue-specific *bantam* expression through multiple enhancer elements that reside up to 20 kb upstream from the CR43334 transcription unit (Slattery et al. 2013). Yki recruits the MLR complex to enhancers to activate transcription of Hippo targets, linking the MLR complex to Hippo signaling and the control of cell proliferation (Oh et al. 2014; Qing et al. 2014). We therefore reasoned that the MLR complex would likely be necessary for proper *bantam* expression and that alteration of *bantam* levels might contribute to the MLR complex depletion phenotypes.

An ancestral genetic split of the full-length MLR methyltransferase generated separate genes in the schizophora dipterans. The Drosophila Cmi (also known as Lpt) gene is homologous to the N-terminal portion and encodes the highly conserved zinc-finger plant homeodomains (PHD) and a high mobility group (HMG) domain (Chauhan et al. 2012). Trithorax-related (Trr) contains the SET domain associated with methyltransferase activity (Sedkov et al. 2003). Despite their split into distinct genes, *Cmi* and *Trr* are essential and both encoded proteins are core components of the Drosophila MLR complex (Chauhan et al. 2012). In this study we modulated the levels of Cmi and Trr in wing and eye precursor tissues, investigated *bantam*'s role in the

resulting phenotypes, and assayed the function of the MLR complex on *bantam* regulation. We found that the MLR complex is bound to tissue-specific *bantam* enhancers and the complex has important functions in regulating the miRNA expression, with both positive and negative effects on *bantam* transcription based on developmental context including tissue type, stage of differentiation, and cell fate. We further demonstrate that the MLR complex has critical enhancer regulatory functions within undifferentiated eye tissue cells that are required for proper *bantam* expression upon subsequent differentiation. Our results suggest that the role of MLR complexes during organismal development is more multifaceted and nuanced than previously reported.

RESULTS

The MLR Complex Genetically Interacts with bantam

We previously reported that modulation of Cmi levels in developing animals leads to a variety of defects, including wing vein pattern disruptions, small and rough eyes, decreased expression of ecdysone hormone regulated genes and effects on organismal growth (Chauhan et al. 2012). In the developing wing *Cmi* depletion leads to retraction of the L2 and L5 longitudinal veins and posterior crossvein (Fig. 1B), while overexpression causes smaller wings with bifurcation of distal veins, as well as ectopic vein formation (Fig. 1C). These phenotypes likely result from alteration of Dpp/Tgf-β signaling (Chauhan et al. 2013). *Cmi* and *Trr* depletion in larval eye discs cause reduction in eye size, while overgrowth is observed at low penetrance with Cmi overexpression (Sedkov et al. 2003; Chauhan et al. 2012). The *Cmi* and *Trr* loss of function phenotypes likely reflect disruptions in gene regulatory networks that control development in response to multiple signaling pathways due to improper enhancer regulation. Indeed, the MLR

complex has been implicated in regulating aspects of the Hippo and Notch pathways as well (Kanda et al. 2013; Oh et al. 2014; Qing et al. 2014).

The Tgf-β, Hippo and Notch pathways share a common regulator, the *bantam* miRNA (Becam et al. 2011; Herranz et al. 2012; Li and Padgett 2012; Attisano and Wrana 2013; Boulan et al. 2013; Zhang et al. 2013; Oh et al. 2014; Qing et al. 2014; Wu et al. 2017; Kane et al. 2018). As *bantam* acts as a negative feedback regulator of Dpp signaling in the wing disc (Kane et al. 2018), we investigated whether the *Cmi* reduced function wing phenotypes were also sensitive to *bantam* levels. Genetic interaction tests between *Cmi* and *bantam* were performed using the Gal4-UAS system expressing transgenic shRNAi or overexpression constructs in the entire larval wing disc. *bantam* activity was increased through overexpression or depleted using a *bantam*-specific miRNA sponge (*ban*-sponge) (Herranz et al. 2012). Simultaneous knockdown of *Cmi* and depletion of *bantam* activity (*C765-Gal4>Cmi-IR,* ban-*sponge*) results in phenotypically wild type wings, demonstrating complete suppression of the short vein phenotype associated with reduced *Cmi* function (Fig. 1E). Conversely, overexpression of *bantam* combined with *Cmi* knockdown results in greater retraction of L2 and L5 veins, thus enhancing the severity of the *Cmi* loss of function phenotype (Fig. 1H). In the background of *Cmi* overexpression (*C765-Gal4>Cmi(OE)*), *bantam* activity depletion leads to an increase in the severity of vein bifurcation and ectopic vein formation (Fig. 1F). Concurrent overexpression of *Cmi* and *bantam* does not appear to suppress the *Cmi* gain-of-function vein phenotype, although wing size is increased to match wild type (Fig. 1I). These data demonstrate that *Cmi* and *bantam* interact genetically and suggest that the alteration of *bantam* levels may be mechanistically involved in the dose dependent *Cmi* wing phenotypes.

Reduced MLR complex function in the Drosophila eye disc results in rough and shrunken adult eyes, including disorganized ommatidia (Sedkov et al. 2003; Chauhan et al. 2012; Kanda et al. 2013). Therefore, we next investigated if the loss of function phenotypes in the eye were sensitive to *bantam* levels. *Eyeless-Gal4* (Ey-Gal4) was used to express *Cmi*- or *Trr*-specific shRNAi constructs in the entire eye pouch of the eye-antennal imaginal disc (*Ey-Gal4>Cmi-IR* and *Ey-Gal4>Trr-IR*) including both undifferentiated and differentiating cells, resulting in phenotypes ranging in severity from small eyes with slight roughness on the posterior margin to near-complete loss of eye tissue (Fig. 2A); *Trr* knockdown phenotypes demonstrated higher penetrance and expressivity compared to *Cmi* knockdown (Fig. 2B). SEM imaging of adult eyes of both knockdown phenotypes revealed disruptions in ommatidial patterning accompanied by bristle loss and duplication, as well as lens fusion (Fig. 2C-E). *Ey-Gal4>bantam* overexpression in the eye disc results in similar pattern disruptions (Fig. 2F), and *bantam* overexpression concurrent with *Cmi-IR* or *Trr-IR* knockdown significantly enhances the rough and shrunken phenotype (Fig. 2B,G-H). Previous studies in which *bantam* was overexpressed exclusively within the differentiating eye have reported similar disruptions of ommatidial patterning due to excess interommatidial cells (Nolo et al. 2006; Thompson and Cohen 2006). Reduction of *bantam* activity via *ban*-sponge expression does not produce a phenotype, yet depletion of *bantam* suppresses the *Cmi* or *Trr* knockdown pattern defects (Fig. 2B,I-K). These data demonstrate that proper *bantam* expression is essential for ommatidial patterning and eye development and suggest that *bantam* dysregulation contributes to the MLR complex loss of function phenotypes.

The MLR Complex Regulates **bantam** *Levels in Developing Tissues*

Our genetic interaction tests reveal a potential role for the MLR complex in regulating the levels of the *bantam* miRNA. To test this hypothesis, we quantitatively measured *bantam* miRNA and its precursor transcript lncRNA:CR43334 by RT-qPCR. *bantam* miRNA is expressed at low levels in late third instar larvae, with broad expression in cells of the wing imaginal disc (Brennecke et al. 2003). We observed increased transcript levels of both the lncRNA precursor and *bantam* miRNA upon depletion of *Cmi* and *Trr* in the wing disc (*C765-Gal4>Cmi-IR* and *C765-Gal4>Trr-IR*) compared to wild type (Fig. 3A). We verified these results using a *bantam* sensor GFP (*ban*sens-GFP) construct that functions as a constitutively expressed inverse reporter of *bantam* activity, such that the higher the expression of *bantam* in a cell, the lower the levels of GFP (see model, Supp. Fig. 1) (Brennecke et al. 2003). Compared to control wing discs and wild type anterior tissue, shRNAi depletion of *Cmi* or *Trr* within the posterior wing compartment using the *En-Gal4* driver results in decreased GFP reporter expression, reflecting increases in *bantam* levels in the developing wing (Fig. 3B). In accordance with the epistatic effects between *Cmi* and *bantam* during wing vein formation (Fig. 1), these data demonstrate that the MLR complex plays a significant role in restricting or negatively regulating *bantam* expression in the developing wing.

The MLR Complex Regulates **bantam** *Expression in a Tissue- and Differentiation-Specific Context*

Based on our genetic interaction phenotypes, we next sought to determine if the MLR complex plays a similar critical regulatory role in controlling *bantam* expression in the developing eye disc. Unlike the wing, in the eye a mobile boundary known as the morphogenetic

furrow induces differentiation as it migrates from the posterior to the anterior margin of the eye pouch, marking the induction of differentiation into separate lineages of proneuronal and interommatidial cells (Supp. Fig. 2). Therefore, tissue anterior to the furrow remains undifferentiated while that posterior to the furrow has begun synchronized differentiation, eventually giving rise to the multiple cell types that will make up the adult compound eye (Cagan 2009). Various Gal4-drivers were used to express *Cmi-IR* and *Trr-IR* in specific cell populations and bantam levels were assayed using the *ban*sens-GFP reporter. *Ey-Gal4* drives expression within the eye pouch but not the antennal section (Fig. 3D); *GawB69B-Gal4* drives expression ubiquitously throughout the entire disc (Fig. 3E); DE-Gal4 drives expression within the dorsal half of the eye pouch, leaving the ventral as an internal wild type control (Fig. 3F); *GMR-Gal4* drives expression only in differentiating tissue posterior to the furrow (Fig. 3G). In wild type eye discs, *bantam* levels remain relatively high in undifferentiated tissue; once differentiation commences, *bantam* is downregulated in proneuronal cells at the center of each developing ommatidia and upregulated in the interommatidial cells bordering the compound eye units (Fig. 3H-I; (Tanaka-Matakatsu et al. 2009)). Regardless of the Gal4 driver, RNAi depletion of either *Cmi* or *Trr* in undifferentiated cells anterior to the morphogenetic furrow does not appreciably alter *bantam* expression in those cells (Fig. 3J-O). However, in *Ey-Gal4, GawB69B-Gal4*, and the dorsal half of *DE-Gal4* discs, *bantam* levels appear to be decreased in differentiating cells, as evidenced by higher GFP sensor signal posterior to the furrow (Fig. 3J-O,R). Surprisingly, *bantam* was expressed at wild-type levels following knockdown of either *Cmi* or *Trr* exclusively in differentiating cells using the *GMR-Gal4* driver (Fig. 3P-R), suggesting that the MLR complex has regulatory function in undifferentiated cells necessary for proper *bantam* expression upon differentiation, but is unnecessary for regulating *bantam* levels once differentiation has

commenced. The downregulation of bantam expression observed in differentiating cells did not appear to be uniform; rather, *bantam* expression appeared to vary by cell type in response to knockdown of *Cmi* and *Trr* (Fig. 3J-O). We therefore sought to more precisely determine whether bantam levels were controlled by the MLR complex in a cell-specific manner. RNAi depletion of *Cmi* or *Trr* throughout the eye pouch using the *Ey-Gal4* driver, revealed that *bantam* is simultaneously upregulated in the differentiating proneuronal ommatidial cells that are positive for Elav staining and downregulated in interommatidial cells (Fig. 3S). Our data reveals that the MLR complex has an important and unexpected role in establishing *bantam* expression levels prospectively in undifferentiated eye cells, and that this epigenetic regulation is necessary for proper cell type specific *bantam* expression in subsequent cell generations in response to differentiation signals.

The MLR Complex Regulates Apoptosis in the Developing Eye

The small and rough eye phenotypes associated with decreased *Cmi* and *Trr* (Fig. 2) suggest elevated apoptosis, decreased proliferation, and/or defects in cellular differentiation. A well characterized function of *bantam* is the inhibition of apoptosis through translational blocking of the proapoptotic *hid* (Grether et al. 1995; Brennecke et al. 2003), and clones of *Trr* mutant cells display small patches of Caspase-3 positive staining (Kanda et al. 2013), implicating apoptotic mechanisms. To address whether elevated apoptosis was involved in the small eye phenotype of *Cmi* and *Trr* knockdown, we stained eye discs for presence of activated effector caspase Dcp-1 (Song et al. 1997). Wild type eye discs undergo sporadic apoptosis in undifferentiated tissue and regulated pruning of cells once the morphogenetic furrow passes and synchronized differentiation commences (Brachmann and Cagan 2003). Knockdown of either *Cmi* or *Trr* in the eye pouch results in increased Dcp-1 activation in the anterior undifferentiated

section of the eye pouch, with a significant concentration of these cells on the dorsal-ventral midline (Fig. 4B,C), the same location identified in *Trr* mutant clones (Kanda et al. 2013). TUNEL staining as a second apoptotic marker confirmed that these cells are undergoing programmed cell death (Supp. Fig. 3A). Knockdown of *Cmi* or *Trr* exclusively in the dorsal eye region via the *DE-Gal4* driver suggests that this effect is cell autonomous (Supp. Fig. 3B). Knockdown of *Cmi* or *Trr* in the posterior margin of the wing using *En-Gal4* demonstrated that the MLR complex's protective effect is conserved in wing tissue (Supp. Fig. 4), although wing discs lack the concentration of apoptotic cells found in undifferentiated eye tissue. To investigate a potential role of *bantam*, Dcp-1 activation was examined in discs overexpressing *bantam* or the *ban*-sponge in the background of *Cmi* or *Trr* knockdown. It has previously been shown that *bantam* overexpression in differentiating eye cells suppresses caspase activation (Thompson and Cohen 2006). Surprisingly, overexpression of the miRNA within the entire eye pouch induces widespread caspase activation in undifferentiated cells, causes overgrowth of the eye pouch, and enhances the Dcp-1 activation phenotype (Fig. 4D-F). Reduction in *bantam* activity through the *ban*-sponge suppresses this phenotype (Fig. 4H-I). Expression of *bantam* anterior to the morphogenetic furrow is not sensitive to levels of *Cmi* or *Trr* (Fig. 3 H-O). Therefore, although it appears that tissue within the undifferentiated eye relies on the MLR complex to prevent cell death, this protective effect does not occur through regulation of *bantam*. Given the fact that both caspase activation in undifferentiated tissue as well as rough and shrunken adult eyes associated with depleted *Cmi* or *Trr* are similarly sensitive to *bantam* levels, we hypothesized that the two are mechanistically linked, and that aberrant cell death in the undifferentiated eye leads to smaller adult organs with patterning defects. To test this, caspase activation in the eye disc was suppressed by expression of p35, a baculovirus substrate inhibitor of caspases including Dcp-1

(Zoog et al. 1999; Song et al. 2000). If increased cell death in undifferentiated eye tissue is mechanistically linked to the rough and shrunken adult eyes, then suppression of apoptosis by p35 should rescue the adult phenotype. Unexpectedly, while p35 successfully reduces apoptotic activation by *Cmi* or *Trr* knockdown (Fig. 4K-L), it significantly enhances the adult phenotypes (Fig. 4M). From these data, we conclude that the rough and shrunken eye phenotype is not a result of the induction of apoptosis in the undifferentiated eye disc. Rather, these are two mechanistically independent phenotypes resulting from the loss of MLR complex activity.

The MLR Complex Directly Modulates **bantam** *Expression Through Enhancer Regulation*

The alteration of *bantam* levels in larval tissues in response to *Cmi* or *Trr* knockdown may be the result of direct or indirect regulatory mechanisms. If the MLR complex directly regulates the expression of *bantam*, it would do so through control of *bantam*-specific enhancers. Such regulatory regions have been identified as necessary and sufficient for transcription factor control of *bantam* locus expression (Oh and Irvine 2011; Slattery et al. 2013). Wing and eye *bantam* enhancer loci have previously been identified as cis-regulatory elements that reside approximately 20kb upstream of the *lncRNA:CR43334* transcription start site (Fig. 5A) (Slattery et al. 2013); enhancer traps of these regions recapitulate the expression pattern of the *bantam* miRNA in the respective imaginal discs, demonstrating tissue-specific regulatory activity. We recently performed Cmi ChIP-sequencing at various developmental stages (Zraly et al., unpublished). Examination of Cmi enrichments near *bantam* revealed localization throughout the locus of the precursor RNA as well as the upstream regulatory region, including peaks at the identified wing and eye enhancers (Fig. 5A). Cmi is absent at these enhancers in the early embryo yet it localizes to both during wandering third instar and prepupal developmental stages, at which point *bantam* is expressed in the imaginal discs. To determine if these binding events

are associated with regulatory activity by the MLR complex, we took advantage of the *LacZ* reporter constructs created to verify the activity patterns of these enhancers (Slattery et al. 2013).

Knockdown of either *Cmi* or *Trr* in the wing lead to increased activity of the *bantam* wing enhancer in the cells normally expressing the miRNA (Fig. 5B). Corresponding with the previous genetic and biochemical data in the wing (Fig. 1, Fig. 3A-B), these data demonstrate that the MLR complex negatively regulates *bantam* expression during wing development through restraints on enhancer activity.

The eye-specific *bantam* enhancer-LacZ reporter demonstrates activity at the very anterior margin of the eye pouch bordering the antennal section. Rather than a clear increase or decrease in activity, upon *Cmi* or *Trr* knockdown this stable pattern is disrupted with sporadic anterior sections of tissue lacking activation and apparent ectopic activation of the enhancer within a wider range of undifferentiated cells (Fig. 5C). These data demonstrate that the MLR complex also directly controls this *bantam* eye enhancer, but its role may be in modulating enhancer activity and restricting activation to certain cells.

Proper enhancer activation requires Nipped-B, which is responsible for loading cohesin to stabilize long-range enhancer/promoter interaction (Rollins et al. 1999; Gause et al. 2008; Gause et al. 2010). Nipped-B interacts with Trr, and the cohesin loading process preferentially recognizes H3K4me1-modified chromatin (Rickels et al. 2017; Yan et al. 2018). If enhancer-mediated regulation of *bantam* underlies the *Cmi* and *Trr* knockdown phenotypes, then we would expect that these phenotypes would be sensitive to levels of Nipped-B in the same way that they are sensitive to *bantam* levels. We have previously shown that depletion of *Nipped-B* enhances the *Cmi* knockdown wing phenotype (Zraly et al, unpublished), just as *bantam* overexpression

does in the *Cmi-IR* background (Fig. 1H). Knockdown of *Nipped-B* results in rough and shrunken eyes phenotypically similar to knockdown of *Cmi* or *Trr,* or overexpression of *bantam*, and both *Cmi* and *Trr* knockdown phenotypes are enhanced by *Nipped-B* knockdown just as they are by *bantam* overexpression (Fig. 2, Fig. S5). These data suggest that the MLR complex's effects on *bantam* expression and organ formation occur through enhancer regulation.

DISCUSSION

We sought to explore *in vivo* mechanisms of target gene regulation by the highly conserved MLR COMPASS-like complex and discovered two key features: 1) We have identified the miRNA *bantam* as an important regulatory target of the Drosophila MLR COMPASS-like complex during tissue development and found that the complex serves to both positively and negatively modulate *bantam* levels depending on cell fate context (Fig. 6). To our knowledge, this is the first example of the MLR COMPASS-like complex regulating a single transcriptional target in opposite directions in different cell types. 2) The MLR complex has important functions in sustaining cell survival and enhancer maintenance in undifferentiated cells.

Reduced MLR complex function results in adult wing and eye phenotypes that reflect dysregulated gene regulatory networks required to drive proper tissue development, including altered signaling pathways that control the time and level of expression of a multitude of target genes. A convergence point among several of these pathways is the microRNA *bantam,* and we found that the *Cmi/Trr* loss of function phenotypes are sensitive to *bantam* levels. Moreover, the MLR complex shows tissue-specific enhancer binding and reduced Cmi/Trr leads to changes in both *bantam* miRNA levels and enhancer activities, suggesting an important and possibly direct

role for the complex in regulating enhancer functions that are activated or silenced in developing tissues. Unexpectedly, reduced *Cmi/Trr* did not lead to reduced *bantam* expression in eye cells once they were committed to differentiate. Rather, in the eye disc the MLR complex has regulatory activity within undifferentiated eye tissue that is necessary for proper *bantam* expression after differentiation commences, suggesting a critical role in enhancer preparation and maintenance.

The MLR complex is highly enriched at the *bantam* locus throughout development where it functions in collaboration with transcription factors, such as Yki, to modulate expression of the lncRNA precursor through the control of tissue-specific enhancers (Slattery et al. 2013). Cmi enrichments are extensive throughout the locus, both upstream and within the lncRNA transcription unit including the *br-C12* regulatory region (Oh and Irvine 2011), suggesting the presence of multiple MLR complex-dependent *bantam* enhancers (Fig. 5). The MLR complex shows temporally targeted enrichment on *bantam* enhancers approximately -20kb from the transcription start site that control both eye and wing expression. While Hippo effector Yki binds to and activates both sequences, binding partner Hth is necessary for regulating the eye enhancer and *bantam* expression in the eye while separate partner Sd is necessary for regulating the wing enhancer and *bantam* expression in the wing (Zhang et al. 2008; Peng et al. 2009; Slattery et al. 2013). Multiple regulatory inputs are necessary for guiding proper spatiotemporal expression of the *bantam* miRNA in imaginal tissue, and our data suggests that the MLR complex plays a critical role in translating these inputs into regulatory decisions.

We previously demonstrated that the Drosophila MLR complex served to positively regulate Dpp signaling during wing vein formation (Chauhan et al. 2013). Our current ChIP-seq results show that Cmi is recruited to a wing-specific *bantam* enhancer during larval development

and we found that reduced levels of MLR complex subunits Cmi and Trr result in both increased activity of this enhancer region and overexpression of *bantam* in the wing disc. These data suggest that the MLR complex is necessary for inhibiting the activity of a target enhancer, a novel function that we have recently also identified at hormone-response elements (Zraly et al., unpublished). The MLR complex is not required to maintain broad *bantam* expression in the larval wing disc and the expression pattern of *bantam* remains unchanged upon knockdown, suggesting that the complex may serve an important function to fine-tune *bantam* levels at this stage of wing development. *bantam* has been identified as a negative regulator of Dpp signaling through translation inhibition of Mad, a downstream effector of Dpp (Kane et al. 2018); thus, the vein patterning defects resulting from decreased Dpp signaling when *Cmi* or *Trr* are depleted may be either exacerbated by or related to elevated *bantam* levels. These results further reveal that proper expression of *bantam* is necessary for correct tissue patterning during wing development, perhaps through regulation of Dpp/Tgf-β signaling.

The RNAi knockdown of *Cmi* and *Trr* in the developing eye tissue produces complex phenotypes, including loss of eye tissue and pattern disruptions of the remaining ommatidia that may result from multiple altered transcriptional targets at various stages of compound eye development. The rough and shrunken phenotype is reminiscent of eye malformations caused by increased cell death or altered developmental signaling (Brennecke et al. 2003; Chao et al. 2004; Nolo et al. 2006), and *bantam* is recognized as both an inhibitor of apoptosis as well as a feedback regulator of multiple signaling pathways (Brennecke et al. 2003; Oh and Irvine 2011; Zhang et al. 2013; Wu et al. 2017; Kane et al. 2018). It has previously been reported that *bantam* overexpression exclusively in the differentiating cells posterior to the morphogenetic furrow during eye development results in eye tissue overgrowth (Nolo et al. 2006; Thompson and Cohen

2006). In contrast, we found that widespread *bantam* expression in the eye disc produced pattern disruptions and reduced organ size similar to loss of *Cmi* and *Trr*, suggesting that changes in developmental signaling rather than growth regulation underlie the eye defects we observed. Through genetic depletion of the MLR complex in different regions of the eye imaginal disc, we found that the complex was not required to maintain *bantam* expression in undifferentiated cells anterior of the morphogenetic furrow; however, the MLR complex has an important role in preparing proper enhancer functions in the undifferentiated cells that will be deployed at the commencement of differentiation after furrow progression. The complex is necessary for the downregulation of *bantam* in proneuronal ommatidial cells destined to give rise to the cone cells and photoreceptors of the adult eye. Simultaneously, the MLR complex is required for *bantam* levels to remain high in the interommatidial cells that develop into the secondary and tertiary pigment cells as well as bristle cells, suggesting that the complex serves to enforce upregulation of the miRNA enhancer in cells of this lineage. Our eye disc studies correlate with *in vitro* data that the Kmt2D MLR complex is dispensable for maintaining gene transcription in murine ESCs, but is required for transcription reprogramming that occurs during differentiation and dedifferentiation (Wang et al. 2016) and perhaps explain why *Cmi/Trr* depletion has no effect on the levels of *bantam* expression in undifferentiated eye tissue. Thus, the critical regulatory function of the MLR complex is presumably to ensure the proper control of *bantam* enhancer activity, either positively or negatively, depending on cell fate during ommatidial formation.

The MLR complex also has an unanticipated role in cell survival. Although the vertebrate and Drosophila MLR (KMT2C, KMT2D and Cmi/Trr) proteins are essential, reduced functions of the vertebrate proteins are associated with developmental disorders and cancers (Fagan and Dingwall 2019) and loss of Trr in eye clones provides a growth advantage versus neighboring

wild type cells (Kanda et al. 2013). Depletion of *Cmi* or *Trr* in the wing disc and in undifferentiated cells of the eye disc results in elevated executioner caspase (Dcp-1) signaling and positive TUNEL staining, indicative of caspase cascade activation and apoptotic cell death. Although apoptosis is important for limiting tissue growth, extensive cell death during tissue development leads to altered organ size (Johnston and Gallant 2002; Fan and Bergmann 2008a);while *Cmi* or *Trr* knockdown in the eye causes shrunken organs, knockdown in the wing causes a modest increase in size (Chauhan et al. 2012). In fact, genetic interaction experiments with caspase inhibitor p35 in the eye demonstrate that cell death is not mechanistically linked to the subsequent rough and shrunken adult eye phenotype, and overexpression of p35 increases the severity of the Cmi and Trr knockdown phenotypes. One potential explanation for these effects is that compensatory proliferation of surviving cells may be able to rescue organ formation through growth signals emanating from the dying cells (James and Bryant 1981; Fan and Bergmann 2008b). Alternatively, the activation of Dcp-1 may promote increased cell growth independent of its role in apoptosis (Song et al. 1997; Shinoda et al. 2019). While caspases are vital for the apoptotic pruning of cells during compound eye formation (Brachmann and Cagan 2003), they also have non-apoptotic developmental function including differentiation regulation of certain cell types (Kuranaga and Miura 2007; Lamkanfi et al. 2007; Nakajima and Kuranaga 2017). Further study will be necessary to identify the transcriptional targets and mechanisms underlying the effects of MLR subunit depletion in the eye disc and adult eye. Importantly, our data demonstrate that the *bantam* miRNA has opposite effects when overexpressed in undifferentiated versus differentiating tissue: when overexpressed within differentiating eye tissue, *bantam* suppresses the caspase cascade (Thompson and Cohen 2006), yet increased levels within undifferentiated cells appear to induce caspase activation. This widespread caspase

activation in undifferentiated eye tissue may not result in complete induction of apoptosis, as it correlates with overgrowth of this section of the eye pouch.

A clearer comprehension of MLR complex roles in enhancer regulation during normal development paves the way to better determine the mechanisms of disease associated with loss of complex functions. The ability to regulate a single transcriptional target in opposite directions depending on tissue type (wing vs. eye) and cell fate choice (proneuronal vs. interommatidial) is critical for normal development. We found that the miRNA *bantam* is an important regulatory target and that the effects of MLR subunit loss on *bantam* expression are dependent on developmental context. While *bantam* has a central role in controlling cell growth and apoptosis during normal development, it has also been shown to be tumorigenic upon overexpression in *Drosophila* cancer models (Sander and Herranz 2019). Potential human counterparts of *bantam* have been identified, including *mir-450b* that has close sequence similarity (Ibanez-Ventoso et al. 2008) and has been described to suppress cancer cell proliferation and induce protective differentiation (Sun et al. 2014; Zhao et al. 2014). The human *mir-130a* can act as either oncogene or tumor suppressor, can impact drug resistance (Zhang et al. 2017), and is functionally related to *bantam* in its feedback regulation of Hippo pathway signaling (Shen et al. 2015). Future studies are needed to address whether these or other miRNAs are conserved regulatory targets of MLR complexes in humans.

MATERIALS AND METHODS

Drosophila Husbandry and Stocks

All stocks and genetic crosses were reared on standard cornmeal/dextrose medium (13% dextrose, 6% yellow cornmeal, 3% yeast extract, 1% agar, 0.3% methylparaben) at 25°C. Experimental crosses were performed at 28°C. *UAS-Cmi-IR, UAS-Trr-IR*, and *UAS-Cmi* lines were previously described (Chauhan et al. 2012). The *UAS-ban*-sponge line was obtained from S. Cohen (Becam et al. 2011). The *bwe-LacZ , bee-LacZ,* and *ban*sens-GFP lines were obtained from R. Mann (Slattery et al. 2013). All other fly strains used in this study were from the Bloomington Drosophila Stock Center (Table S1) and are described in Flybase (http://flybase.bio.indiana.edu).

Imaginal Disc Preparation, Immunofluorescence, and Imaging

Wandering third instar larvae were collected and imaginal discs dissected in ice-cold PBS, fixed in 4% formaldehyde in PBS for 15-20 minutes, then washed in PBST (PBS + 0.1% Triton X-100) three times for 5 minutes each. Washed tissues were then blocked in PBSTB (PBST + 0.1% BSA) for two hours at room temperature followed by incubation in the primary antibody diluted in PBSTB overnight at 4°C. After incubation, tissues were washed twice in PBSTB for 5 minutes each, once in PBSTB + 2% NGS for 30 minutes, and then twice more in PBSTB for 15 minutes each, followed by incubation in secondary antibody diluted in PBSTB in the dark for 1 hour at room temperature. Tissues were washed three times in PBST for 5 minutes each, then mounted in ProLong Gold antifade reagent with DAPI (Invitrogen).

Primary antibodies included mouse α-β-Gal (JIE7) and mouse α-Elav (9F8A9) (Developmental Studies Hybridoma Bank/Univ. of Iowa), rabbit α-GFP (GenScript) and rabbit

α-Dcp-1 (Asp216) (Cell Signaling Technologies). Guinea pig α-Cmi was generated as previously described (Chauhan et al. 2012). Primary antibodies were used at 1:1000 concentration, except α-Dcp-1 was used at 1:250 concentration. Secondary antibodies were used at 1:1000 concentration and included α-Mouse, α-Rabbit, and α-Guinea Pig IgG (H+L) conjugated to Alexafluor 488 or 568 fluorophores (Life Technologies). Compound microscopy images were captured using an Olympus BX53 microscope with a Hamamatsu ORCA Flash 4.0 LT camera. Confocal microscopy images were captured using a Zeiss LSM 880 Airyscan and processed using Zeiss Zen® software. Quantification of GFP signal mean fluorescence intensity was assayed using Fiji ImageJ software to measure fluorescence intensity as mean grey value of selected areas, subtracting background (Schindelin et al. 2012).

Scanning Electron Microscopy

Adult eyes were prepared for scanning electron microscopy using critical point drying as previously described (Wolff 2011). SEM photography was taken at 1500X magnification using a Hitachi SU3500 microscope.

Adult Wing Preparation, Mounting, and Imaging

Wings were dissected from adult animals and dehydrated in isopropyl alcohol for 20 minutes. After dehydration, wings were mounted in DPX mountant (Fluka). Images were captured using a Leica MZ16 microscope with Leica DFC480 camera.

ChIP-seq

Chromatin from whole animals was collected, prepared, and analyzed according to (Zraly et al., unpublished).

miRNA extraction, cDNA synthesis and qRT-PCR

Wing discs from 50 Drosophila third instar larvae of the appropriate genotype were dissected and miRNA was prepared using the miRVana isolation kit (Life technologies) to enrich for small RNAs, according to manufacturer's protocols. RNA (10ng) was reverse transcribed using Multiscribe reverse transcriptase (ThermoFisher Scientific) and TaqMan small RNA assay RT primers specific for bantam (Assay ID: 000331) and 2S RNA (Assay ID: 001766; control), according to manufacturer's protocols. For qRT-PCR of miRNAs, TaqMan Universal PCR Master Mix II (No UNG, ThermoFisher Scientific) and miRNA-specific TaqMan microRNA Assay was used. To enrich for long RNAs, total RNA was also isolated using the miRVana kit according to manufacturer's protocols. The RNA was DNase digested, and reverse transcribed, as previously described (Chauhan et al. 2013). The primer sequences used to amplify *bantam* precursor, CR43334 are as follows: Forward primer: 5'-GCGATGTATGCGTGTAGTTAAAG-3'; Reverse primer: 5'-CCACTTTGTCGATCGTTTCATG-3'. Real time qPCR was performed on a QuantStudio6 Flex Real Time PCR System (BioRad). The $2^{-\Delta\Delta CT}$ method was used for quantification.

Statistical Analysis

Significant difference of eye phenotype severity between genetic populations was measured using Pearson's Chi-Squared Test. Significant difference of mean fluorescence intensity in eye and wing discs was measured using Student's T-test.

Acknowledgements

We thank Manuel O. Diaz and Richard Schultz for helpful discussions and comments on the manuscript, Jordan Beach and the SSOM Department of Cell and Molecular Physiology Specialized Imaging Resource Center for use of the Zeiss LSM 880 Airyscan microscope, and Michael Sertwetnyk for assistance with Drosophila genetic analyses. Fly stocks were obtained from the Bloomington Drosophila Stock Center, supported by the National Institutes of Health (P40OD018537) and from Stephen Cohen and Richard Mann. SEM analyses were performed with the help of Joseph Schluep and Jacob Ciszek at the Loyola University Chicago SEM facility, supported by a grant from the National Science Foundation-Major Research Instrumentation (MRI) Program [1726994].

Competing interests

The authors declare that there are no competing interests.

Funding

The research was supported by grants from the National Science Foundation [MCB-1413331 and MCB-1716431 to A.K.D.].

References

Andersen EC, Horvitz HR. 2007. Two C. elegans histone methyltransferases repress lin-3 EGF transcription to inhibit vulval development. *Development* **134**: 2991-2999.

Ang SY, Uebersohn A, Spencer CI, Huang Y, Lee JE, Ge K, Bruneau BG. 2016. KMT2D regulates specific programs in heart development via histone H3 lysine 4 di-methylation. *Development* **143**: 810-821.

Attisano L, Wrana JL. 2013. Signal integration in TGF-beta, WNT, and Hippo pathways. *F1000Prime Rep* **5**: 17.

Becam I, Rafel N, Hong X, Cohen SM, Milan M. 2011. Notch-mediated repression of bantam miRNA contributes to boundary formation in the Drosophila wing. *Development* **138**: 3781-3789.

Boulan L, Martin D, Milan M. 2013. bantam miRNA promotes systemic growth by connecting insulin signaling and ecdysone production. *Curr Biol* **23**: 473-478.

Brachmann CB, Cagan RL. 2003. Patterning the fly eye: the role of apoptosis. *Trends Genet* **19**: 91-96.

Brennecke J, Hipfner DR, Stark A, Russell RB, Cohen SM. 2003. bantam encodes a developmentally regulated microRNA that controls cell proliferation and regulates the proapoptotic gene hid in Drosophila. *Cell* **113**: 25-36.

Cagan R. 2009. Principles of Drosophila eye differentiation. *Curr Top Dev Biol* **89**: 115-135.

Chao JL, Tsai YC, Chiu SJ, Sun YH. 2004. Localized Notch signal acts through eyg and upd to promote global growth in Drosophila eye. *Development* **131**: 3839-3847.

Chauhan C, Zraly CB, Dingwall AK. 2013. The Drosophila COMPASS-like Cmi-Trr coactivator complex regulates dpp/BMP signaling in pattern formation. *Developmental Biology* **380**: 185-198.

Chauhan C, Zraly CB, Parilla M, Diaz MO, Dingwall AK. 2012. Histone recognition and nuclear receptor co-activator functions of Drosophila Cara Mitad, a homolog of the N-terminal portion of mammalian MLL2 and MLL3. *Development* **139**: 1997-2008.

Fagan RJ, Dingwall AK. 2019. COMPASS Ascending: Emerging clues regarding the roles of MLL3/KMT2C and MLL2/KMT2D proteins in cancer. *Cancer Lett* **458**: 56-65.

Fan Y, Bergmann A. 2008a. Apoptosis-induced compensatory proliferation. The Cell is dead. Long live the Cell! *Trends Cell Biol* **18**: 467-473.

Fan Y, Bergmann A. 2008b. Distinct mechanisms of apoptosis-induced compensatory proliferation in proliferating and differentiating tissues in the Drosophila eye. *Dev Cell* **14**: 399-410.

Ford DJ, Dingwall AK. 2015. The cancer COMPASS: navigating the functions of MLL complexes in cancer. *Cancer Genet* **208**: 178-191.

Gause M, Misulovin Z, Bilyeu A, Dorsett D. 2010. Dosage-sensitive regulation of cohesin chromosome binding and dynamics by Nipped-B, Pds5, and Wapl. *Mol Cell Biol* **30**: 4940-4951.

Gause M, Schaaf CA, Dorsett D. 2008. Cohesin and CTCF: cooperating to control chromosome conformation? *Bioessays* **30**: 715-718.

Grether ME, Abrams JM, Agapite J, White K, Steller H. 1995. The head involution defective gene of Drosophila melanogaster functions in programmed cell death. *Genes Dev* **9**: 1694-1708.

Herranz H, Hong X, Cohen SM. 2012. Mutual repression by bantam miRNA and Capicua links the EGFR/MAPK and Hippo pathways in growth control. *Curr Biol* **22**: 651-657.

Herz HM, Mohan M, Garruss AS, Liang K, Takahashi YH, Mickey K, Voets O, Verrijzer CP, Shilatifard A. 2012. Enhancer-associated H3K4 monomethylation by Trithorax-related, the Drosophila homolog of mammalian Mll3/Mll4. *Genes Dev* **26**: 2604-2620.

Hipfner DR, Weigmann K, Cohen SM. 2002. The bantam gene regulates Drosophila growth. *Genetics* **161**: 1527-1537.

Hu D, Garruss AS, Gao X, Morgan MA, Cook M, Smith ER, Shilatifard A. 2013. The Mll2 branch of the COMPASS family regulates bivalent promoters in mouse embryonic stem cells. *Nat Struct Mol Biol* **20**: 1093-1097.

Ibanez-Ventoso C, Vora M, Driscoll M. 2008. Sequence relationships among C. elegans, D. melanogaster and human microRNAs highlight the extensive conservation of microRNAs in biology. *PLoS One* **3**: e2818.

Issaeva I, Zonis Y, Rozovskaia T, Orlovsky K, Croce CM, Nakamura T, Mazo A, Eisenbach L, Canaani E. 2007. Knockdown of ALR (MLL2) reveals ALR target genes and leads to alterations in cell adhesion and growth. *Mol Cell Biol* **27**: 1889-1903.

James AA, Bryant PJ. 1981. A quantitative study of cell death and mitotic inhibition in gamma-irradiated imaginal wing discs of Drosophila melanogaster. *Radiat Res* **87**: 552-564.

Johnston LA, Gallant P. 2002. Control of growth and organ size in Drosophila. *Bioessays* **24**: 54-64.

Kanda H, Nguyen A, Chen L, Okano H, Hariharan IK. 2013. The Drosophila ortholog of MLL3 and MLL4, trithorax related, functions as a negative regulator of tissue growth. *Mol Cell Biol* **33**: 1702-1710.

Kane NS, Vora M, Padgett RW, Li Y. 2018. bantam microRNA is a negative regulator of the Drosophila decapentaplegic pathway. *Fly (Austin)* **12**: 105-117.

Kleefstra T, Kramer JM, Neveling K, Willemsen MH, Koemans TS, Vissers LE, Wissink-Lindhout W, Fenckova M, van den Akker WM, Kasri NN et al. 2012. Disruption of an EHMT1-associated chromatin-modification module causes intellectual disability. *American journal of human genetics* **91**: 73-82.

Kuranaga E, Miura M. 2007. Nonapoptotic functions of caspases: caspases as regulatory molecules for immunity and cell-fate determination. *Trends Cell Biol* **17**: 135-144.

Lai B, Lee JE, Jang Y, Wang L, Peng W, Ge K. 2017. MLL3/MLL4 are required for CBP/p300 binding on enhancers and super-enhancer formation in brown adipogenesis. *Nucleic Acids Res* **45**: 6388-6403.

Lamkanfi M, Festjens N, Declercq W, Vanden Berghe T, Vandenabeele P. 2007. Caspases in cell survival, proliferation and differentiation. *Cell Death Differ* **14**: 44-55.

Lee JE, Wang C, Xu S, Cho YW, Wang L, Feng X, Baldridge A, Sartorelli V, Zhuang L, Peng W et al. 2013. H3K4 mono- and di-methyltransferase MLL4 is required for enhancer activation during cell differentiation. *Elife* **2**: e01503.

Levine M. 2010. Transcriptional enhancers in animal development and evolution. *Curr Biol* **20**: R754-763.

Li Y, Padgett RW. 2012. bantam is required for optic lobe development and glial cell proliferation. *PLoS One* **7**: e32910.

Nakajima YI, Kuranaga E. 2017. Caspase-dependent non-apoptotic processes in development. *Cell Death Differ* **24**: 1422-1430.

Nan Z, Yang W, Lyu J, Wang F, Deng Q, Xi Y, Yang X, Ge W. 2019. Drosophila Hcf regulates the Hippo signaling pathway via association with the histone H3K4 methyltransferase Trr. *Biochem J* **476**: 759-768.

Ng SB, Bigham AW, Buckingham KJ, Hannibal MC, McMillin MJ, Gildersleeve HI, Beck AE, Tabor HK, Cooper GM, Mefford HC et al. 2010. Exome sequencing identifies MLL2 mutations as a cause of Kabuki syndrome. *Nat Genet* **42**: 790-793.

Nolo R, Morrison CM, Tao C, Zhang X, Halder G. 2006. The bantam microRNA is a target of the hippo tumor-suppressor pathway. *Current biology : CB* **16**: 1895-1904.

Oh H, Irvine KD. 2011. Cooperative regulation of growth by Yorkie and Mad through bantam. *Developmental cell* **20**: 109-122.

Oh H, Slattery M, Ma L, Crofts A, White KP, Mann RS, Irvine KD. 2013. Genome-wide association of Yorkie with chromatin and chromatin-remodeling complexes. *Cell Rep* **3**: 309-318.

Oh H, Slattery M, Ma L, White KP, Mann RS, Irvine KD. 2014. Yorkie promotes transcription by recruiting a histone methyltransferase complex. *Cell Rep* **8**: 449-459.

Oswald F, Rodriguez P, Giaimo BD, Antonello ZA, Mira L, Mittler G, Thiel VN, Collins KJ, Tabaja N, Cizelsky W et al. 2016. A phospho-dependent mechanism involving NCoR and KMT2D controls a permissive chromatin state at Notch target genes. *Nucleic Acids Res*.

Peng HW, Slattery M, Mann RS. 2009. Transcription factor choice in the Hippo signaling pathway: homothorax and yorkie regulation of the microRNA bantam in the progenitor domain of the Drosophila eye imaginal disc. *Genes Dev* **23**: 2307-2319.

Qing Y, Yin F, Wang W, Zheng Y, Guo P, Schozer F, Deng H, Pan D. 2014. The Hippo effector Yorkie activates transcription by interacting with a histone methyltransferase complex through Ncoa6. *Elife* **3**.

Rickels R, Herz HM, Sze CC, Cao K, Morgan MA, Collings CK, Gause M, Takahashi YH, Wang L, Rendleman EJ et al. 2017. Histone H3K4 monomethylation catalyzed by Trr and mammalian COMPASS-like proteins at enhancers is dispensable for development and viability. *Nat Genet* **49**: 1647-1653.

Rollins RA, Morcillo P, Dorsett D. 1999. Nipped-B, a Drosophila homologue of chromosomal adherins, participates in activation by remote enhancers in the cut and Ultrabithorax genes. *Genetics* **152**: 577-593.

Sander M, Herranz H. 2019. MicroRNAs in Drosophila Cancer Models. *Adv Exp Med Biol* **1167**: 157-173.

Schindelin J, Arganda-Carreras I, Frise E, Kaynig V, Longair M, Pietzsch T, Preibisch S, Rueden C, Saalfeld S, Schmid B et al. 2012. Fiji: an open-source platform for biological-image analysis. *Nat Methods* **9**: 676-682.

Sedkov Y, Benes JJ, Berger JR, Riker KM, Tillib S, Jones RS, Mazo A. 1999. Molecular genetic analysis of the Drosophila trithorax-related gene which encodes a novel SET domain protein. *Mech Dev* **82**: 171-179.

Sedkov Y, Cho E, Petruk S, Cherbas L, Smith ST, Jones RS, Cherbas P, Canaani E, Jaynes JB, Mazo A. 2003. Methylation at lysine 4 of histone H3 in ecdysone-dependent development of Drosophila. *Nature* **426**: 78-83.

Shen S, Guo X, Yan H, Lu Y, Ji X, Li L, Liang T, Zhou D, Feng XH, Zhao JC et al. 2015. A miR-130a-YAP positive feedback loop promotes organ size and tumorigenesis. *Cell Res* **25**: 997-1012.

Shilatifard A. 2012. The COMPASS family of histone H3K4 methylases: mechanisms of regulation in development and disease pathogenesis. *Annu Rev Biochem* **81**: 65-95.
Shinoda N, Hanawa N, Chihara T, Koto A, Miura M. 2019. Dronc-independent basal executioner caspase activity sustains Drosophila imaginal tissue growth. *Proc Natl Acad Sci U S A* **116**: 20539-20544.
Slattery M, Voutev R, Ma L, Negre N, White KP, Mann RS. 2013. Divergent transcriptional regulatory logic at the intersection of tissue growth and developmental patterning. *PLoS Genet* **9**: e1003753.
Song Z, Guan B, Bergman A, Nicholson DW, Thornberry NA, Peterson EP, Steller H. 2000. Biochemical and genetic interactions between Drosophila caspases and the proapoptotic genes rpr, hid, and grim. *Mol Cell Biol* **20**: 2907-2914.
Song Z, McCall K, Steller H. 1997. DCP-1, a Drosophila cell death protease essential for development. *Science* **275**: 536-540.
Sun MM, Li JF, Guo LL, Xiao HT, Dong L, Wang F, Huang FB, Cao D, Qin T, Yin XH et al. 2014. TGF-beta1 suppression of microRNA-450b-5p expression: a novel mechanism for blocking myogenic differentiation of rhabdomyosarcoma. *Oncogene* **33**: 2075-2086.
Tanaka-Matakatsu M, Xu J, Cheng L, Du W. 2009. Regulation of apoptosis of rbf mutant cells during Drosophila development. *Dev Biol* **326**: 347-356.
Thompson BJ, Cohen SM. 2006. The Hippo pathway regulates the bantam microRNA to control cell proliferation and apoptosis in Drosophila. *Cell* **126**: 767-774.
Van Laarhoven PM, Neitzel LR, Quintana AM, Geiger EA, Zackai EH, Clouthier DE, Artinger KB, Ming JE, Shaikh TH. 2015. Kabuki syndrome genes KMT2D and KDM6A: functional analyses demonstrate critical roles in craniofacial, heart and brain development. *Hum Mol Genet* **24**: 4443-4453.
Wang C, Lee JE, Lai B, Macfarlan TS, Xu S, Zhuang L, Liu C, Peng W, Ge K. 2016. Enhancer priming by H3K4 methyltransferase MLL4 controls cell fate transition. *Proc Natl Acad Sci U S A* **113**: 11871-11876.
Wolff T. 2011. Preparation of Drosophila eye specimens for scanning electron microscopy. *Cold Spring Harb Protoc* **2011**: 1383-1385.
Wu YC, Lee KS, Song Y, Gehrke S, Lu B. 2017. The bantam microRNA acts through Numb to exert cell growth control and feedback regulation of Notch in tumor-forming stem cells in the Drosophila brain. *PLoS Genet* **13**: e1006785.
Yan J, Chen SA, Local A, Liu T, Qiu Y, Dorighi KM, Preissl S, Rivera CM, Wang C, Ye Z et al. 2018. Histone H3 lysine 4 monomethylation modulates long-range chromatin interactions at enhancers. *Cell Res* **28**: 204-220.
Zhang HD, Jiang LH, Sun DW, Li J, Ji ZL. 2017. The role of miR-130a in cancer. *Breast Cancer* **24**: 521-527.
Zhang L, Ren F, Zhang Q, Chen Y, Wang B, Jiang J. 2008. The TEAD/TEF family of transcription factor Scalloped mediates Hippo signaling in organ size control. *Dev Cell* **14**: 377-387.
Zhang X, Luo D, Pflugfelder GO, Shen J. 2013. Dpp signaling inhibits proliferation in the Drosophila wing by Omb-dependent regional control of bantam. *Development* **140**: 2917-2922.
Zhao Z, Li R, Sha S, Wang Q, Mao W, Liu T. 2014. Targeting HER3 with miR-450b-3p suppresses breast cancer cells proliferation. *Cancer Biol Ther* **15**: 1404-1412.

Zoog SJ, Bertin J, Friesen PD. 1999. Caspase inhibition by baculovirus P35 requires interaction between the reactive site loop and the beta-sheet core. *J Biol Chem* **274**: 25995-26002.

FIGURE LEGENDS

Figure 1.

The MLR complex genetically interacts with bantam during wing development. *C765-Gal4* was used to drive expression of genetic constructs modulating levels of *Cmi* or *bantam* in the wing disc. Compared to wild type wings (A), knockdown of *Cmi (Cmi-IR)* (B) causes retraction of wing veins, most commonly L2 and L5. (C) *Cmi* overexpression results in smaller wings and ectopic distal veins. (D) Reduction of *bantam* activity via expression of a *bantam*-specific miRNA sponge (UAS-*ban*-sponge) does not alter adult wing phenotype. (E) *bantam* reduction in the background of *Cmi* depletion completely rescues the wild type phenotype. (F) *bantam* reduction alongside *Cmi* overexpression enhances the phenotype, causing ectopic vein formation. (G) Overexpressing *bantam* during wing formation causes end vein bifurcation of L5. (H) *bantam* overexpression in parallel with *Cmi* knockdown enhances the *Cmi* loss-of-function phenotype. (I) Overexpression of both *Cmi* and *bantam* results in enhanced vein bifurcation, crossvein retraction, and recues wing size. Black arrows highlight vein formation defects.

Figure 2.

The MLR complex genetically interacts with bantam during eye development. *Ey-Gal4* was used to drive expression of genetic constructs modulating levels of *Cmi, Trr*, or *bantam* in the eye disc. (A) Knockdown of *Cmi* or *Trr* during eye development results in rough and shrunken eyes that range in penetrance and expressivity. (B) Adults of the listed genotypes were scored according to eye phenotype severity; N > 50 for all genotypes; ** = $p \leq 0.01$. Overexpression of *bantam* significantly enhances the *Cmi* or *Trr* knockdown phenotypes, while reduction of *bantam* activity using the *ban*-sponge suppresses the Cmi knockdown phenotype.

Overexpression of *bantam* alone causes slightly rough and shrunken eyes; expression of the *ban*-sponge alone has no phenotypic effect. (C-K) SEM images of adult compound eyes demonstrate roughness is due to ommatidial patterning defects. As compared to wild type ommatidia (C), Cmi knockdown (D) and Trr knockdown (E) eyes display ommatidial crowding, lens fusion, and bristle loss and duplication. This is also seen when *bantam* is overexpressed alone (F), in the Cmi-IR background (G), and the Trr-IR background (H). (I) Reduction of *bantam* activity has no effect on ommatidial patterning and appears to suppress the effect of Cmi (J) or Trr (K) knockdown.

Figure 3.

The MLR complex regulates bantam expression. (A) RT-qPCR was performed on whole wing discs. Both the *bantam* precursor *lncRNA:CR43334* and processed *bantam* miRNA are upregulated upon *Cmi* or *Trr* knockdown. (B) *En-Gal4* was used to knockdown *Cmi* or *Trr* in the posterior wing disc; a *bantam*-GFP inverse sensor construct was used to compare *bantam* miRNA levels between posterior (P) and anterior (A) of organ. (Left) Tissue in the posterior of *En-Gal4>Cmi-IR* and *En-Gal4>Trr-IR* organs demonstrate increased *bantam* levels (lower GFP). (Right) posterior/anterior ratio of *bantam* sensor signal quantified; ** = $p \leq 0.01$. (C-G) *Cmi* was knocked down using various Gal4 drivers to visualize driver expression pattern. Expression of these drivers is visualized by immunostaining Cmi (green) and Elav (red), which labels proneuronal cells posterior to the morphogenetic furrow. (C) *Ey-Gal4* drives knockdown within the eye pouch. (D) *GawB69B-Gal4* drives ubiquitously throughout the organ. (E) *DE-Gal4* drives only within the dorsal half of the eye pouch. (F) *GMR-Gal4* drives only posterior to the morphogenetic furrow. (H-Q) The *bantam*-GFP inverse sensor construct (*ban*sens-GFP) was used to assay *bantam* miRNA levels. Magnified views of developing ommatidia posterior to the

furrow are displayed to the right of each eye disc. *bantam* levels in the undifferentiated anterior tissue anterior to the furrow remain unchanged in all genotypes. (H-I) In control discs, *bantam* levels are relatively high anterior to the furrow (low GFP) and lower posterior (high GFP). (J-O) When *Cmi* or *Trr* is depleted both anterior and posterior to the furrow (*Ey-Gal4, GawB69B-Gal4*, and *DE-Gal4*), *bantam* levels appear to decrease in the differentiating posterior tissue. (P-Q) If *Cmi/Trr* are depleted only within this differentiating tissue using *GMR>Gal4*, *bantam* levels remain unchanged compared to control. (R) Mean fluorescence intensity anterior to the furrow was quantified from cohorts of each genotype; N ≥ 10 for all genotypes; * = p≤0.05, ** = p≤0.01, NS = not significant. (S) Developing ommatidia in eye discs were stained for proneuronal marker Elav (red) and *ban*sens-GFP (green). Control organs demonstrate colocalization of GFP and Elav. Upon knockdown of either *Cmi* or *Trr* using *Ey-Gal4*, changes in *bantam* expression vary by cell fate. In proneuronal cells *bantam* levels are increased (lower GFP), and in interommatidial cells bantam levels are decreased (higher GFP).

Figure 4.

The MLR complex suppresses caspase activation in the undifferentiated eye. Expression of shRNAi knockdown or overexpression constructs was driven in the eye disc using *Ey-Gal4*. Apoptosis in the eye disc was assayed by staining for cleaved effector caspase Dcp-1 (green). The morphogenetic furrow is marked by a thick dotted line and the discs are outlined by a thin dotted line. (A) Wild type eye discs demonstrate low sporadic caspase activation. (B-C) Knockdown of *Cmi* or *Trr* in the eye pouch using *Ey-Gal4* results in increased caspase activity in undifferentiated cells. This activity in concentrated in a cluster of apoptotic cells on the dorsal-ventral midline anterior to the morphogenetic furrow. (D) Overexpression of *bantam* causes eye pouch overgrowth and caspase activation in undifferentiated tissue. (E-F) Increased *bantam*

expression in the background of *Cmi/Trr* knockdown enhances caspase activation. While reduction of *bantam* activity through expression of the *ban*-sponge has no effects on caspase activation (G), it suppresses the apoptotic induction of *Cmi/Trr*-depleted organs (H-I). (J) Caspase inhibitor p35 represses caspase activation. (K-L) p35 expression alongside *Cmi/Trr* knockdown suppresses the caspase phenotype. (M) Adult eye phenotype was scored and quantified. p35 expression phenocopies the rough and shrunken phenotype of *Cmi/Trr* knockdown and enhances the phenotype in a *Cmi/Trr* knockdown background; ** = $p \leq 0.01$. Simultaneous *Trr* knockdown and p35 overexpression results in synthetic lethality; therefore, statistical significance between *Trr-IR* and *Trr-IR;p35* not achieved due to a low number of surviving adults.

Figure 5.

The MLR complex localizes to and regulates tissue-specific bantam enhancers. ChIP-seq was used to assay binding of MLR subunit Cmi across the *bantam*-containing lncRNA locus as well as at upstream tissue-specific enhancer regions. Binding profiles across different developmental timepoints including early embryo, wandering third-instar larva, and white prepupa, demonstrate consistent localization of the complex to the lncRNA locus as well as previously identified eye- and wing-specific enhancer regions (Slattery et al. 2013) during imaginal disc development. (B) *Cmi* or *Trr* was knocked down throughout the wing disc using *C765-Gal4*; a *bantam* wing enhancer-β-Gal reporter (*bwe-LacZ*) was used to compare enhancer activity levels. *C765-Gal4>Cmi-IR* and *C765-Gal4>Trr-IR* discs demonstrate increased *bantam* wing enhancer activity levels compared to control. (C) *Cmi* or *Trr* were knocked down throughout the eye pouch of the eye disc using *Ey-Gal4*. A *bantam* eye enhancer-β-Gal reporter (*bee-LacZ*) was

used to compare enhancer activity levels. *Ey-Gal4>Cmi-IR* and *Ey-Gal4>Trr-IR* organs demonstrated disrupted *bantam* eye enhancer activity patterns compared to control.

Figure 6.

Model of MLR complex functions in tissue development. The Drosophila MLR COMPASS-like complex may either have positive or negative regulatory activity on the miRNA *bantam* depending on the context of cell fate. Tissue-specific *bantam* enhancers active in undifferentiated wing or eye tissue are bound and regulated by MLR. In the wing disc, MLR represses the activity of the *bantam* wing enhancer and downregulates *bantam* miRNA. In the eye disc, MLR modulates the expression pattern of the *bantam* eye enhancer in undifferentiated cells. After passage of the morphogenetic furrow and cell fate choice between proneuronal or interommatidial lineages, the previous regulatory activity of MLR leads to increased *bantam* expression in the proneuronal cells and decreased expression in the interommatidial cells.

Figure 1

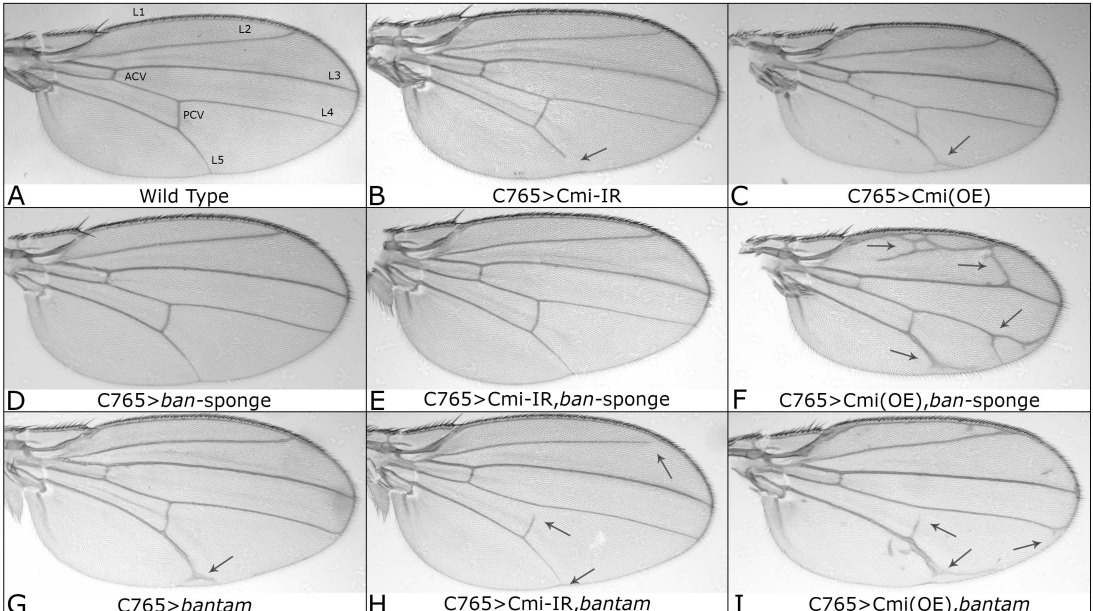
L1
L2
ACV
L3
PCV
L4
L5
A Wild Type
B C765>Cmi-IR
C C765>Cmi(OE)
D C765>*ban*-sponge
E C765>Cmi-IR,*ban*-sponge
F C765>Cmi(OE),*ban*-sponge
G C765>*bantam*
H C765>Cmi-IR,*bantam*
I C765>Cmi(OE),*bantam*

Figure 2

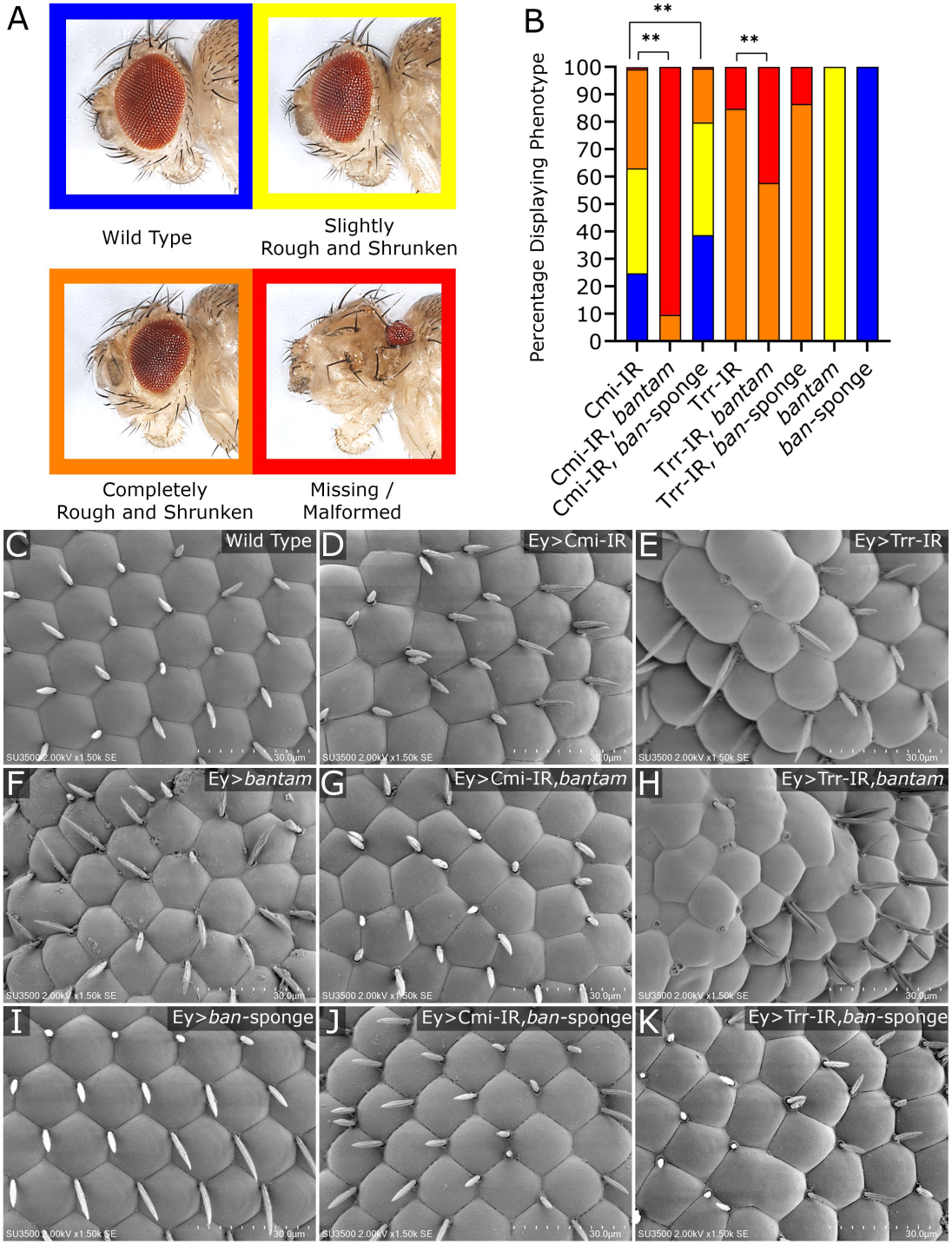
A
Wild Type
Slightly Rough and Shrunken
Completely Rough and Shrunken
Missing / Malformed
B
Percentage Displaying Phenotype
100
90
80
70
60
50
40
30
20
10
0
**
**
**
Cmi-IR
Cmi-IR, bantam
Cmi-IR, ban-sponge
Trr-IR
Trr-IR, bantam
Trr-IR, ban-sponge
bantam
ban-sponge
C Wild Type
D Ey>Cmi-IR
E Ey>Trr-IR
F Ey>bantam
G Ey>Cmi-IR,bantam
H Ey>Trr-IR,bantam
I Ey>ban-sponge
J Ey>Cmi-IR,ban-sponge
K Ey>Trr-IR,ban-sponge

Figure 3

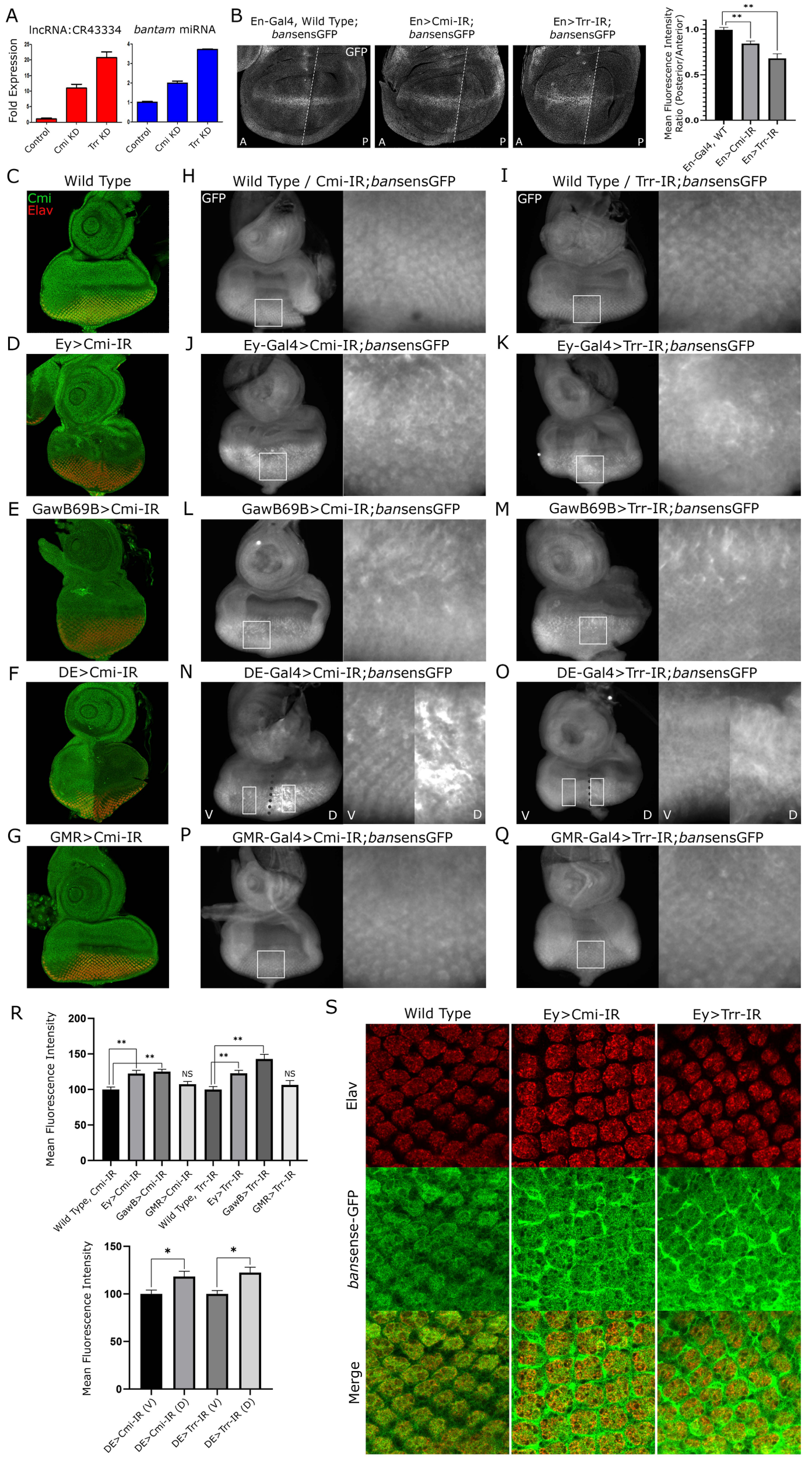
A
lncRNA:CR43334
bantam miRNA
Fold Expression
Control
Cmi KD
Trr KD
B
En-Gal4, Wild Type; bansensGFP
En>Cmi-IR; bansensGFP
En>Trr-IR; bansensGFP
GFP
A
P
Mean Fluorescence Intensity Ratio (Posterior/Anterior)
En-Gal4, WT
En>Cmi-IR
En>Trr-IR
C
Wild Type
Cmi
Elav
H
Wild Type / Cmi-IR;bansensGFP
I
Wild Type / Trr-IR;bansensGFP
D
Ey>Cmi-IR
J
Ey-Gal4>Cmi-IR;bansensGFP
K
Ey-Gal4>Trr-IR;bansensGFP
E
GawB69B>Cmi-IR
L
GawB69B>Cmi-IR;bansensGFP
M
GawB69B>Trr-IR;bansensGFP
F
DE>Cmi-IR
N
DE-Gal4>Cmi-IR;bansensGFP
O
DE-Gal4>Trr-IR;bansensGFP
V
D
G
GMR>Cmi-IR
P
GMR-Gal4>Cmi-IR;bansensGFP
Q
GMR-Gal4>Trr-IR;bansensGFP
R
Mean Fluorescence Intensity
Wild Type, Cmi-IR
Ey>Cmi-IR
GawB>Cmi-IR
GMR>Cmi-IR
Wild Type, Trr-IR
Ey>Trr-IR
GawB>Trr-IR
GMR>Trr-IR
NS
DE>Cmi-IR (V)
DE>Cmi-IR (D)
DE>Trr-IR (V)
DE>Trr-IR (D)
S
Wild Type
Ey>Cmi-IR
Ey>Trr-IR
Elav
bansense-GFP
Merge

Figure 4

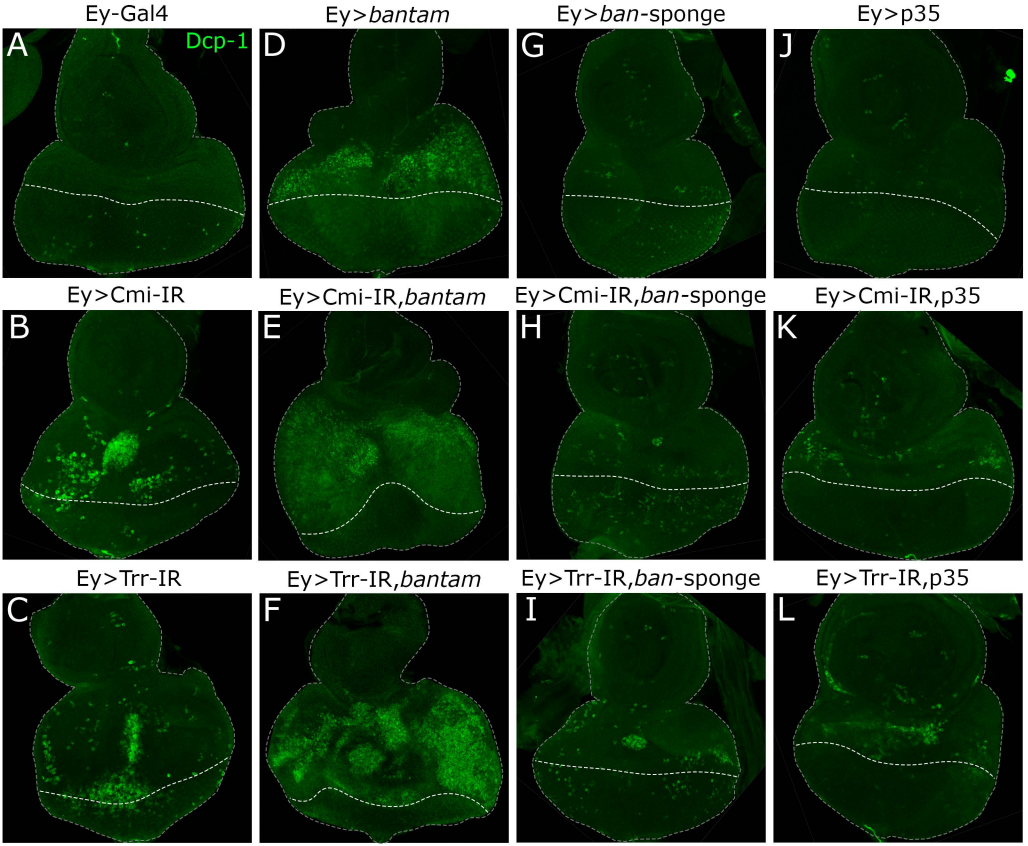
Ey-Gal4
Ey>*bantam*
Ey>*ban*-sponge
Ey>p35
A
Dcp-1
D
G
J
Ey>Cmi-IR
Ey>Cmi-IR,*bantam*
Ey>Cmi-IR,*ban*-sponge
Ey>Cmi-IR,p35
B
E
H
K
Ey>Trr-IR
Ey>Trr-IR,*bantam*
Ey>Trr-IR,*ban*-sponge
Ey>Trr-IR,p35
C
F
I
L

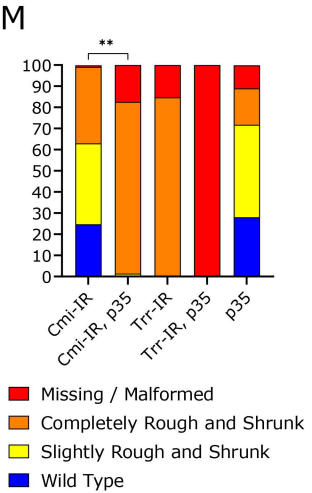
M
**
100
90
80
70
60
50
40
30
20
10
0
Cmi-IR
Cmi-IR, p35
Trr-IR
Trr-IR, p35
p35
Missing / Malformed
Completely Rough and Shrunk
Slightly Rough and Shrunk
Wild Type

Figure 5

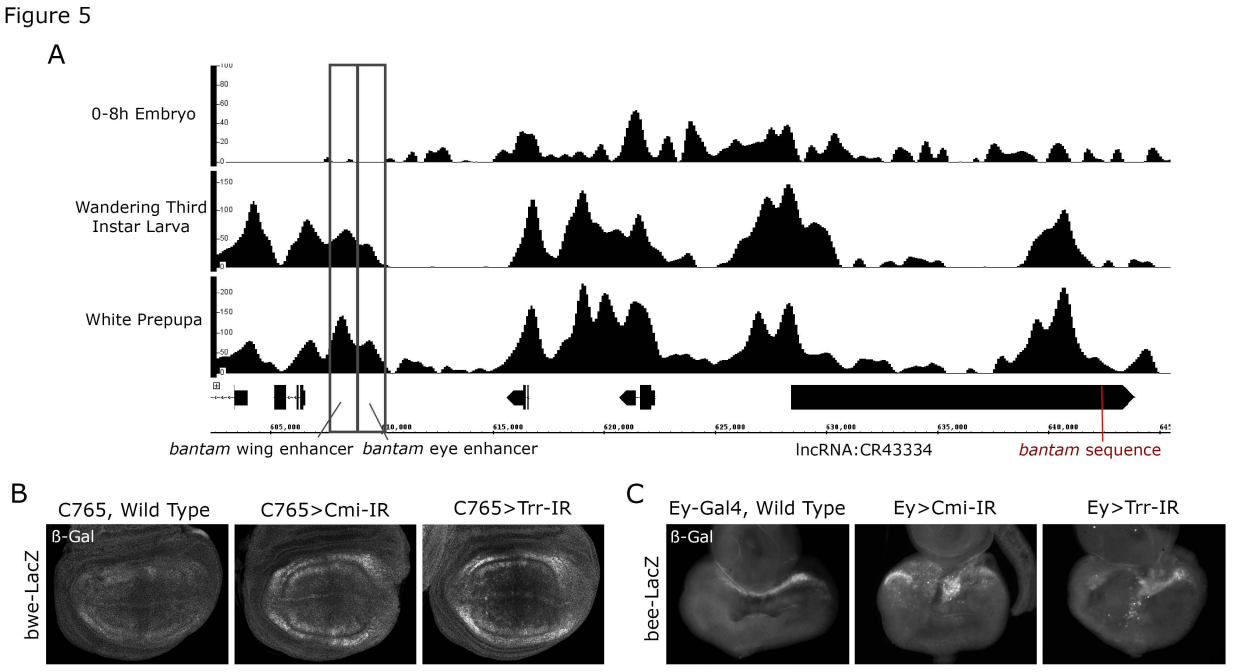
A
0-8h Embryo
Wandering Third Instar Larva
White Prepupa
bantam wing enhancer
bantam eye enhancer
lncRNA:CR43334
bantam sequence
B
C765, Wild Type
C765>Cmi-IR
C765>Trr-IR
ß-Gal
bwe-LacZ
C
Ey-Gal4, Wild Type
Ey>Cmi-IR
Ey>Trr-IR
ß-Gal
bee-LacZ

Figure 6

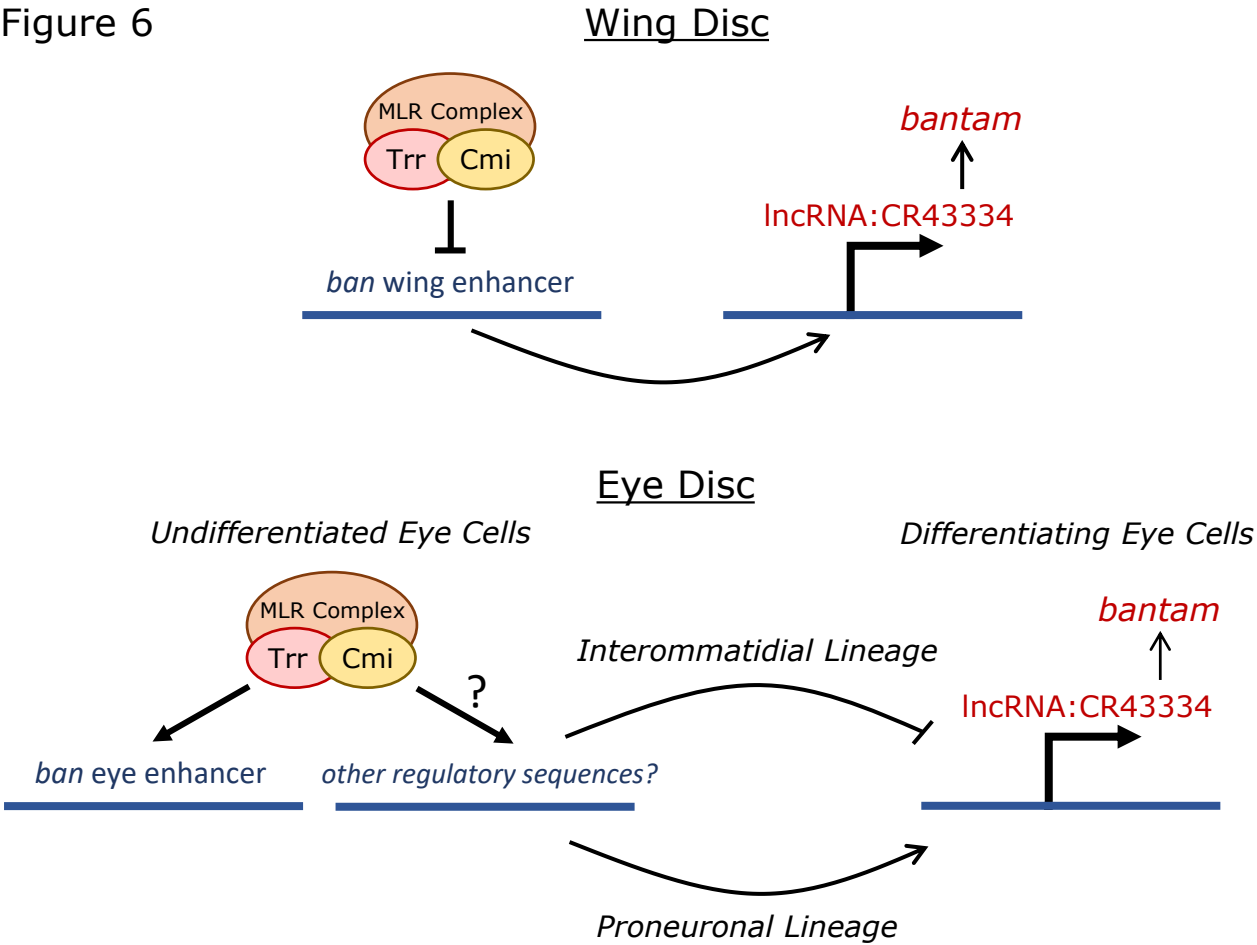
Wing Disc
MLR Complex
Trr
Cmi
bantam
lncRNA:CR43334
ban wing enhancer
Eye Disc
Undifferentiated Eye Cells
Differentiating Eye Cells
MLR Complex
Trr
Cmi
?
Interommatidial Lineage
bantam
lncRNA:CR43334
ban eye enhancer
other regulatory sequences?
Proneuronal Lineage